Photon-stimulated desorption of neutrals from silver and alkali halides

H. Kanzaki and T. Mori
Institute for Solid State Physics, The University of Tokyo, Roppongi, Minato-ku, Tokyo 106, Japan
(Received 8 November 1983)

Photon-stimulated desorption (PSD) from silver and alkali halides under valence excitation is studied by a sensitive method in which the desorption rate is measured by lock-in detection of a mass-spectrometer signal under chopped excitation. Main results are as follows. (a) The main desorption species are identified as halogen molecules in silver halides (AgBr and AgCl), and alkali-metal and halogen atoms in alkali halides (RbBr, KI, and RbI). (b) The decay time of the desorption rate corresponds to the lifetime τ of the relevant photoexcited states. The molecular desorption from silver halides, in contrast to the atomic desorption from alkali halides, results in a unique decay behavior in silver halides such as the decrease of τ with increasing excitation intensity. (c) Temperature dependence of the desorption yield under weakly absorbed photon excitation corresponds to that of $(D\tau)^{1/2}$ (with D, the diffusion coefficient of the excited states), except at the low-temperature threshold (-85 °C) in AgBr, which is determined by the surface adsorption energy of Br_2. (d) Desorption-yield spectra of silver halides are well described in terms of the diffusion of excited states and give the value of $D\tau$ at various temperatures. Combined with τ, we can estimate D, which is 1×10^{-6} cm^2 sec^{-1} for AgBr at room temperature. From these results, the diffusion of relevant excited states is shown to be important in the PSD under valence excitation, and models for diffusing species are proposed.

I. INTRODUCTION

The study of desorption of neutrals and ions from a solid surface induced by electronic excitation has two aspects: one is to explore the energy transfer mechanism at the surface, and the other is to obtain information on the surface species.[1] Concerning the first aspect, a number of studies have been made on electron-stimulated desorption (ESD) from alkali halides, and the results are interpreted in relation to the defect-formation mechanism.[2–4] On the other hand, only a few studies on this aspect[5,6] are concerned with photon-stimulated desorption (PSD) from ionic crystals. Recently, desorption of excited alkali atoms from alkali halides has been observed in both ESD and PSD experiments.[7] As for the second aspect, the recent proposal of a core-Auger mechanism for ion desorption[8] stimulated a variety of photon-stimulated ion-desorption (PSID) experiments using synchrotron radiation and opened up a new approach in surface study.[9]

The present work deals with the PSD under excitation near the fundamental absorption edge in silver and alkali halides. This is in contrast to the previous studies mentioned above, most of which are interested in high-energy excited states including core-level excitations. The PSD study under low-energy valence excitation is of main concern in this work and has been initiated in order to achieve deeper understanding of the PSD process, which is one of the important channels in the relaxation of excited states in solids. In this context, the comparison between silver and alkali halides will be interesting, because the two materials are known to behave quite differently in the relaxation of excited electronic states.[10]

Basically, the present study is an extension of Luckey's work[6] on halogen evolution from silver halides under ultraviolet irradiation. By using newly developed experimental techniques, we succeeded in observing much more details of the PSD process than hitherto possible, such as the mass-spectroscopic identification of desorbed species, the desorption kinetics, and the dependence of desorption yield on both temperature and incident-photon energy. The results obtained clearly indicate that the diffusion of photoexcited species toward the surface plays an important role in the PSD process under valence excitation. Thus it turned out that PSD is a unique technique for the transport study of photoexcited states, especially when it is difficult by other experimental methods.

An outline of experimental results was briefly reported previously,[11] and a full account of the work will be given in the present paper. In the following, the experimental techniques are described in Sec. II. In Sec. III experimental results and discussion are presented for silver and alkali halides. Main conclusions are summarized in Sec. IV.

II. EXPERIMENTAL TECHNIQUES

Figure 1 illustrates a schematic diagram of the experimental arrangement. A sample in the vacuum chamber is irradiated through a sapphire window by excitation light chopped at a frequency between 2 and 10^3 Hz. The species desorbed from the sample surface are electron-bombarded (typically 70 eV, 200 μA) during their flight across the ionizer. The positive ions thus produced are analyzed by a quadrupole mass spectrometer (Anelva NAG-536). The output signal from the electron multiplier in the mass spectrometer is modulated with a frequency of chopped excitation and the modulated component is measured by a lock-in amplifier (Princeton Applied Research model 121). The overall response time of

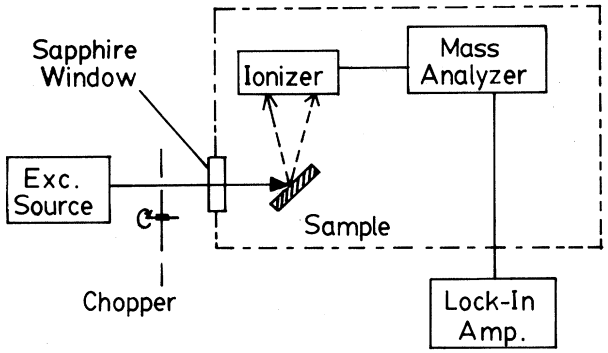

FIG. 1. Schematic diagram of experimental arrangement for PSD studies.

the measuring system, including the time of flight of both the desorbed species and the ionized positive ions, can be estimated as less than 10^{-4} sec. Thus the output of the lock-in amplifier at the chopping-frequency range is proportional to the amplitude of the modulated component of the desorption rate.

Several features of the present method are noticeable. Firstly, a remarkable improvement of the signal-to-noise ratio, at least 10^3, is achieved by the present technique, in comparison with the usual method in which a change of mass spectra by sample irradiation is measured.[12] Secondly, the present method measures the desorption rate, not the integrated amount of desorbed species during the irradiation period, and the detection sensitivity is not influenced by the accumulation of desorbed species in vacuum caused by previous irradiation. In addition, the species remaining in vacuum after irradiation are usually different from the desorption species, as will be shown in Sec. III A. Thirdly, as will be shown in Sec. III B, the present method can give information on the desorption kinetics by studying the dependence of desorption rate on the chopping frequency of excitation.

As the excitation light source, a quartz-iodine lamp (Ushio JC-24-150, 24 V, 6 A maximum) is used for most of the studies (in Secs. III A, III B, and III C) on silver halides, in combination with a band-pass filter (Toshiba UV-D36A) with a transmission peak at 360 nm. The excitation corresponds to the indirect band-to-band transition of the silver halides. The absorption coefficients of the silver halides at room temperature for 360 nm are 5×10^3 and $3\times10^3\,\mathrm{cm}^{-1}$, for AgBr and AgCl, respectively. For the excitation spectroscopy of silver halides (in Sec. III D), a xenon-short-arc lamp (Osram 75 W, 14 V, 5.4 A) is used in combination with a Leiss single monochromator equipped with a Suprasil prism. For alkali halides, total radiation from either a xenon-short-arc or a deuterium lamp (HTV-L544, 85 V, 0.3 A) is used. The wavelength range effective for excitation of alkali halides is estimated from absorption spectra of the sample. The shortest wavelength is limited at 195 nm because of absorption by both a Suprasil lens and a sapphire window in the light path. The effective absorption coefficient of RbBr is estimated to be approximately $10^3\,\mathrm{cm}^{-1}$, corresponding to the tail of the lowest exciton absorption.

The excitation-light intensity is varied either by changing the source current or by inserting calibrated nickel screens in the light path. The photon flux incident on the sample is measured by using a calibrated thermopile.

Silver halide crystals are prepared by zone-refining in halogen atmosphere. The method of sample preparation has been described previously.[13] Samples of 2-mm-thick crystals are chemically polished by KCN solution, washed in distilled water, and annealed at 250 °C in a clean vacuum of 10^{-6} Torr before mounting in the sample holder. Alkali halide crystals are either grown at the Crystal Growth Laboratory of the University of Utah (RbBr and RbI) or obtained from Harshaw Chemical Co. (KI). They are cleaved in dry air and quickly transferred to the vacuum chamber.

The vacuum chamber, made of stainless steel, is evacuated by an ion getter pump and all the PSD experiments are carried out in vacuum better than 1×10^{-8} Torr after baking at 250 °C. Sample crystals are mounted on a sample holder attached to a cold finger of a variable-temperature cryostat. The temperature can be varied between 80 and 600 K. As indicated in Fig. 1, the excitation light is incident on the sample surface with an angle of 45°. The distance between sample and ionizer is approximately 35 mm, and the ionizer accepted the desorbed species emitted within solid angle of 5×10^{-2} sr along the direction perpendicular to the excitation light.

Because of the destructive nature of the desorption experiment, damage effects due to excessive irradiation are expected. In the present study, the damage effects are always observed as the decrease of the desorption rate. However, it is found that the desorption rate does not change appreciably (reduction of less than 10%) when the integrated amount of exposure is below a certain limit. In silver halides at room temperature (in Secs. III A and III B), the exposure of less than 10^{17} quanta cm^{-2} of 360-nm light is the safety range. In silver halides at low temperatures (in Secs. III C and III D), the limitation is more severe and special precautions are required. In alkali halides the amount of maximum allowable exposure is found to be less. Except as otherwise stated, the data which showed appreciable decrease of the desorption rate are disregarded.

III. RESULTS AND DISCUSSION

A. Identification of desorption species

Figure 2 shows typical mass spectra of PSD species. As will be described, the relative intensities of various mass signals for the same sample are independent of temperature, excitation intensity, and chopping frequency of excitation.

Under all the experimental conditions studied, the mass signal is reduced to less than 1×10^{-3} when electron bombardment in the ionizer is turned off. This observation indicates that the desorbed species do not contain positive ions. The present apparatus cannot detect negative ions, and the possible desorption of a small amount of negative ions cannot be denied, in view of negative ion desorption (in addition to neutrals) reported for alkali halides under laser excitation[5] or during thermal desorption after low-

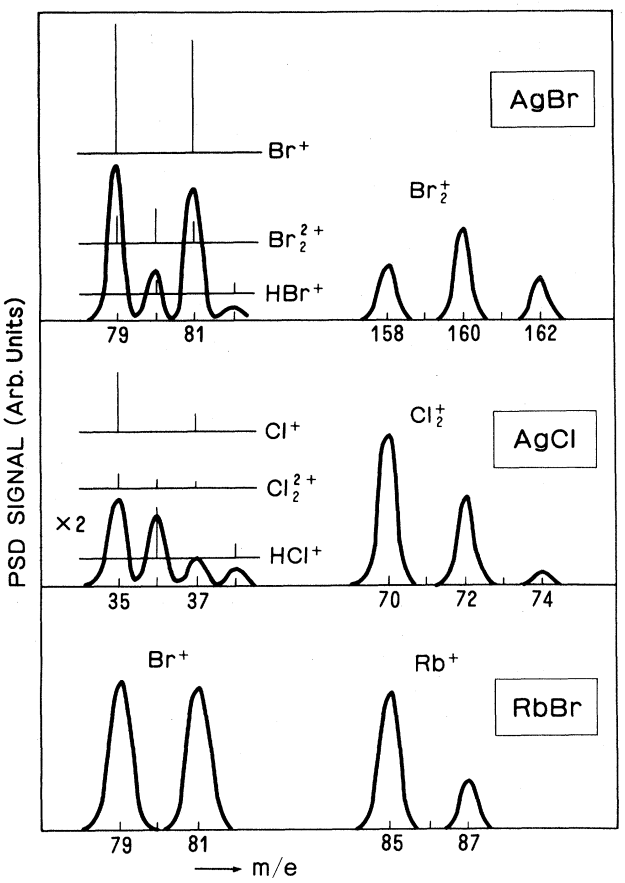

FIG. 2. Typical mass spectra of PSD species from silver and alkali halides at room temperature. Mass peaks in silver halides at smaller (m/e) values are composites, and the constituents, as indicated, are identified on the basis of a natural abundance ratio of isotopes.

temperature irradiation.[14] However, we can reasonably conclude that the majority of desorbed species detected in the present study are desorbed from the sample surface as neutrals and then ionized during their flight in the ionizer. This conclusion agrees with previous results showing that the majority of desorbed species in ESD and PSD of alkali halides are neutrals.[2,7]

Some of the mass peaks for silver halides in Fig. 2 are composites. On the basis of the natural abundance ratio of isotopes, we can identify the constituents in a consistent way and the results are shown in Fig. 2. Take, for example, the mass spectrum for AgBr. The mass peaks (158, 160, and 162) are solely due to Br_2^+ and their intensity ratio is precisely as expected from the abundance ratio of isotopes. On the other hand, the mass peak 79 includes both Br^+ and Br_2^{2+}: 80 for $(HBr)^+$ and Br_2^{2+}, 81 for Br^+ and Br_2^{2+}, and 82 for $(HBr)^+$. At this point, possible candidates for the desorption species are Br_2, Br, and HBr in AgBr, and similarly in AgCl.

The situation is simple for RbBr in Fig. 2. Alkali and halogen atoms can be concluded as the desorption species for all alkali halides studied: RbBr, RbI, and KI. In contrast to ESD results,[15] desorption of halogen molecules is not observed in the present study. In the early stage of study on RbBr, $(HBr)^+$ was sometimes observed in addition to Rb^+ and Br^+. It was found later that a thorough baking of sample can remove the $(HBr)^+$ signal completely. A possible origin of HBr desorption from RbBr may be the H_2O molecule adsorbed at the surface. On the other hand, however, the desorption of hydrogen halides from silver halides is not reduced by further baking. It may be that some hydrogen-containing species are strongly adsorbed on silver halides and produce HBr or HCl by reaction with photogenerated halogens.

An important question for PSD in silver halides is whether the basic desorption species are halogen atoms and/or halogen molecules. There are two alternatives which can explain the results shown in Fig. 2. One is that both atoms and molecules are desorbed and the molecule is formed by the association of atoms at the surface. This seems the situation of molecular desorption under electron irradiation of alkali halides.[15] The other is that only the molecule is desorbed and the halogen ion is produced by electron bombardment of the molecule in the ionizer. The experimental results relevant to this question are as follows: (1) The intensity ratio of molecule to atom does not change in varying the excitation intensity by 20:1, and (2) the intensity ratio does not change in the temperature range studied, −85 °C to 80 °C for AgBr and −40 °C to 130 °C for AgCl. These results are consistent only with the second possibility mentioned above, because the association of atoms to molecules in the first alternative will depend on both excitation intensity and temperature.[15] We can thus conclude that the halogen molecule is the main desorption species in silver halides and the halogen ions observed are produced in the ionizer.

It is found that the species which remain in vacuum after irradiation are different from the desorption species. For example, the main species which remain after irradiation of silver halides are hydrogen halides (HX), halogen atoms (X), and very few halogen molecules (X_2). In the mass spectra of the remaining species, the $(HX)^+$ signals are much stronger than X^+ and the relative ratio is reversed to that in the case of PSD species such as shown in Fig. 2. The observation agrees with the previous report in which an increase of $(HCl)^+$ and Cl^+ is observed in mass spectra after electron irradiation of AgCl.[16] The situation may be that the desorbed HX remains in the vacuum space longer than X_2, and the X^+ is produced from HX in the ionizer.

In the following, we will discuss the difference of desorption species between silver and alkali halides. As far as the main species are concerned, we concluded that only halogen molecules are desorbed from silver halides. On the other hand, both alkali-metal and halogen atoms are desorbed from the alkali halides studied.

Photoexcitation in the present study corresponds to the optical transition of the lowest valence-excitation, in both silver and alkali halides. We postulate that the desorption under such low-energy excitation is mostly the evaporation of species with nearly thermal kinetic energy. If this is the case, the desorption is equivalent to the evaporation of molecules or atoms adsorbed at the surface. Then, in the case of intrinsic desorption (desorption of constituents of the bulk material), the "precursor" for desorption which is adsorbed at the surface corresponds to the local-

ized electrons or holes located at the surface, the wave function of which is possibly in the range of atomic or molecular dimension. One of the conditions required for the precursor to be actually desorbed will be that its binding energy to the surface should be sufficiently small in comparison to thermal energy kT.

As for the desorption of metallic elements such as alkali metals or silver, there has been an empirical relation observed in previous studies, namely, the desorption of atoms for metals with lower vapor pressure,[3] which is less efficient. The observation of no silver desorption from silver halides is certainly along the line of the empirical rule, in comparison with desorption observed for rubidium or potassium from alkali halides. Although no quantitative estimate is yet available, we can reasonably understand these observations in terms of the dependence of desorption efficiency on the magnitude of surface binding energy mentioned above.

The experimental result that halogen atoms are desorbed from alkali halides but not from silver halides is extremely interesting. The difference observed between silver and alkali halides suggests that a halogen atom (a positive hole localized at a surface halide ion) can be efficiently desorbed from alkali halides but not from silver halides. We propose the following interpretation on the basis of a difference in the property of localized electronic states between silver and alkali halides.

The localized states in silver halides, in general, are much shallower than those in alkali halides.[10] In order that the precursor state can be desorbed, there will be a certain condition for its degree of localization. Suppose the existence of a very shallow localized precursor state with a diffuse wave function. The effective vapor pressure of such precursor will not be so different from the vapor pressure of the bulk material, and its desorption will be very inefficient. The wave function of a hole localized at a halogen atom will be more diffuse than that of localized holes at a diatomic halogen molecule because of the formation of a bonding orbital during the association of atoms to form a molecule. A possible reason for the observed difference may be that wave function of a localized hole at a halogen atom is sufficiently localized in alkali halides for the desorption to occur, but not sufficient in silver halides. In silver halides the formation of diatomic molecule is required for the sufficient localization necessary for efficient desorption.

B. Desorption kinetics

In order to study desorption kinetics, the modulated desorption rate is measured as a function of the chopping frequency of excitation under various excitation intensities. Results of desorption rate versus chopping frequency are shown in Figs. 3 and 4 for the silver and alkali halides, respectively. It is noticeable that the desorption rate decreases systematically by increasing chopping frequency in both silver and alkali halides. The observed dependence on chopping frequency can be understood in terms of the decay of the desorption rate. Assuming an exponential time decay of the desorption rate after pulse excitation, the frequency dependence of the desorption rate R_{desorp} measured in the present experiment can be given by

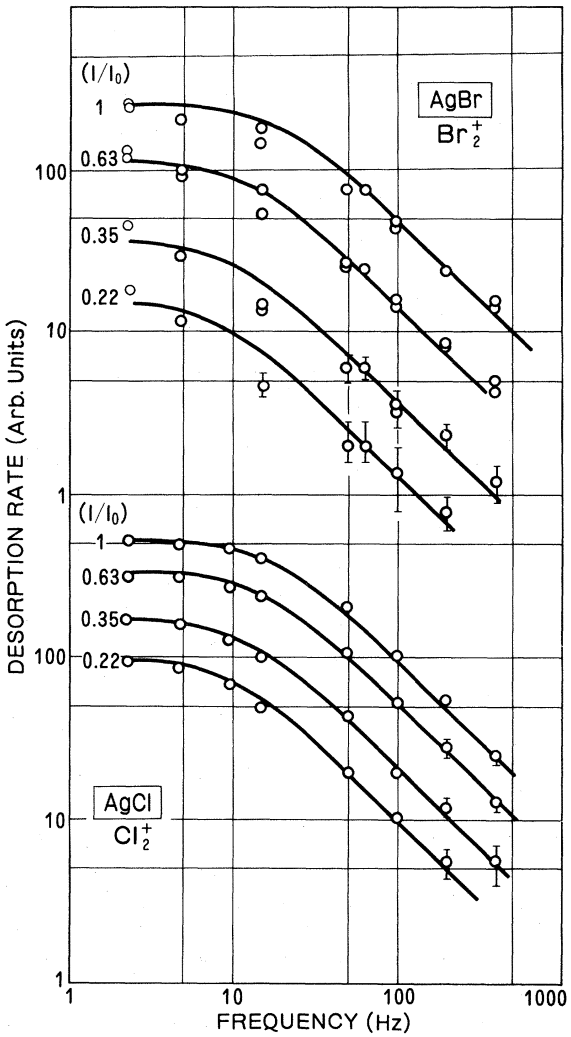

FIG. 3. PSD rate of halogen molecule vs chopping frequency of excitation under various excitation intensities I, for silver halides at 25 °C. Excitation intensity I_0 corresponds to 4×10^{15} and 5×10^{15} quanta $\text{cm}^{-2}\,\text{sec}^{-1}$, for AgBr and AgCl, respectively. Curves represent the best fit of data to Eq. (1).

$$R_{\text{desorp}} \propto [1+(\omega\tau)^2]^{-1/2}\,, \tag{1}$$

where ω is the angular frequency of excitation and τ is the desorption decay time. As indicated in Figs. 3 and 4, the results of fitting the experimental data to Eq. (1) are satisfactory enough to evaluate the decay time. The values of τ thus obtained are summarized in Table I. The decay time changes with excitation intensity in silver halides, but not in alkali halides.

The decay times obtained for RbBr are close to those observed in ESD of RbBr by Overeijnder *et al.*[17] They measured both the decay time and the kinetic-energy distribution of desorbed neutrals. They obtained the decay time for the main desorption component as follows: $(2.5\pm0.5)\times10^{-3}$ sec for rubidium and $(0.5\pm0.2)\times10^{-3}$ sec for bromine, both of which are identified as the decay of desorbed atoms with thermal kinetic energies. Although the kinetic-energy distribution is not measured in the present study, the above agreement suggests that the desorbed neutrals in the present PSD study are thermally

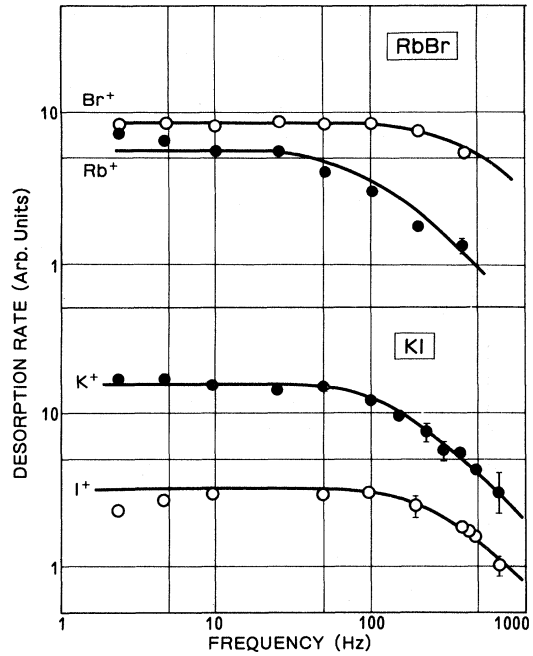

FIG. 4. PSD rate of alkali and halogen atoms vs chopping frequency of excitation for RbBr and KI at 25 °C. Curves represent the best fit of data to Eq. (1).

TABLE I. Desorption decay time τ at 25 °C obtained from the dependence of desorption rate on chopping frequency under various excitation intensities. Optical excitation is at 360 nm for silver halides, and at wavelengths longer than 200 nm for alkali halides.

Crystal	Desorption species	Incident photon flux (quanta $cm^{-2} sec^{-1}$)	τ (10^{-3} sec)
AgBr	Br_2	4×10^{15}	9.9±1.5
		$4\times0.63\times10^{15}$	13.3±2.6
		$4\times0.35\times10^{15}$	18.6±4.1
		$4\times0.22\times10^{15}$	26 ±6
AgCl	Cl_2	5×10^{15}	8.7±0.7
		$5\times0.63\times10^{15}$	10.4±1.0
		$5\times0.35\times10^{15}$	13.4±1.2
		$5\times0.22\times10^{15}$	16.1±1.6
RbBr	Rb	9.5×10^{13}	2.2±0.5
	Br	9.5×10^{13}	0.4±0.1
KI	K	4.3×10^{14}	1.2±0.3
	I	4.3×10^{14}	0.7±0.1

desorbed from the surface. Furthermore, desorption with the long decay time of 10^{-3}–10^{-2} sec given in Table I will be consistent with the thermal desorption process.[17]

The decay times measured for halogen-ion signals (X^+) in silver halides are found the same as those for halogen molecular ions (X_2^+) under the same excitation intensity, within experimental accuracy. This is consistent with the conclusion in Sec. III A that the main desorption species in silver halides are halogen molecules.

The variation of decay time with excitation intensity in silver halides is related to the change of the "excitation intensity dependence of the desorption rate" with chopping frequency. Figure 5 shows the desorption rate versus excitation intensity I for various chopping frequencies in silver halides. General behavior noticeable in Fig. 5 can be summarized as follows. Firstly,

$$R_{\text{desorp}} \propto I \tag{2}$$

at lower chopping frequencies and under higher excitation intensities, and secondly,

$$R_{\text{desorp}} \propto I^2 \tag{3}$$

at higher chopping frequencies and under lower excitation intensities.

Contrary to silver halides, a simple desorption behavior is observed for the alkali halides. The decay time does not depend on the excitation intensity as far as the range of present study indicates, and

$$R_{\text{desorp}} \propto I\ , \tag{4}$$

irrespective of chopping frequency, as shown in Fig. 6.

In the following, discussion will start on the origin of the decay time and then on the difference in desorption kinetics between silver and alkali halides. Possible candidates for the origin of the desorption decay time will be as follows: (a) residence time of the desorption species at the surface, (b) decay time required for the diffusion of photoexcited species to the surface, and (c) lifetime of the photoexcited species.

Firstly, on the basis of the temperature-dependence study on AgBr and RbBr in Sec. III C, it can be concluded that the desorption at room temperature occurs instantly when the desorption species (or desorption precursors in Sec. III A) are located at the surface. This excludes the possibility (a) as far as the decay time at room temperature is concerned, and secondly, effects of the diffusion time (b) could be considerable in the present excitation by weakly absorbed photons. Assuming the one-dimensional diffusion of the photoexcited species towards the surface,[18] the decay of the desorption rate solely due to the diffusion time will be given by

$$R_{\text{desorp}} \approx (D/\pi t)^{1/2} \tag{5}$$

for weakly absorbed photons, where D is the diffusion coefficient of the photoexcited species and t is the time after the pulse excitation. Such a time decay as Eq. (5) results in the chopping-frequency dependence as

$$R_{\text{desorp}} \propto \omega^{-1/2}\ , \tag{6}$$

which is different from Eq. (1). In view of the agreement of experimental results with Eq. (1), we can conclude that the diffusion time is not a main origin of the decay time. On the other hand, the decay of the desorption rate due to the finite lifetime τ of the photoexcited species will be given by

$$R_{\text{desorp}} \propto \exp(-t/\tau)\ , \tag{7}$$

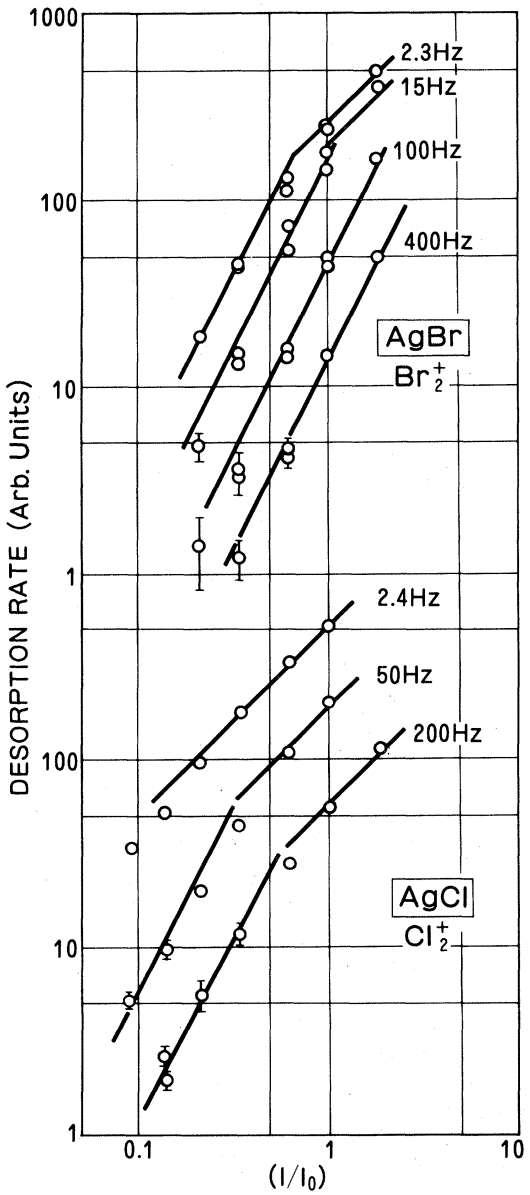

FIG. 5. PSD rate of halogen molecule vs excitation intensity for various chopping frequencies in silver halides at 25 °C. The magnitude of I_0 is the same as Fig. 3. The slope of straight lines is either 1 or 2.

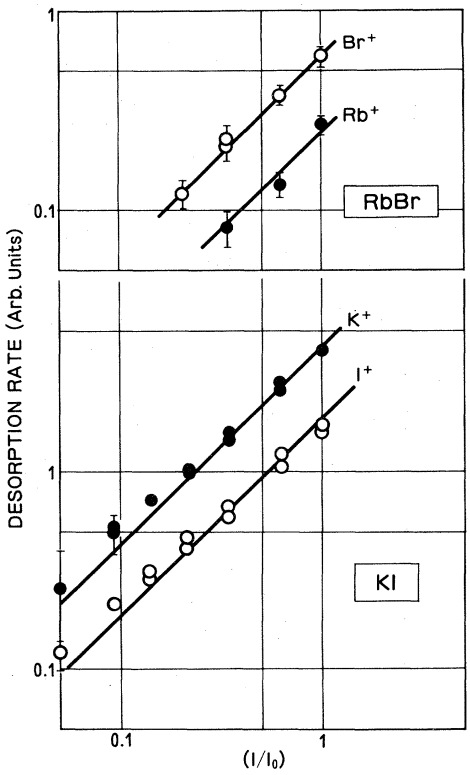

FIG. 6. PSD rate vs excitation intensity for alkali halides at 25 °C. Values of I_0 are 9.5×10^{13} and 4.3×10^{14} quanta cm^{-2} sec^{-1} for RbBr and KI, respectively.

which leads to the behavior expressed by Eq. (1). Thus we can conclude that the decay time we observed is mainly determined by the lifetime of the photoexcited species.

The decay time in silver halides at room temperature is 1×10^{-2} sec in Table I, which is much longer than the lifetime of free holes in AgBr, 1×10^{-5} sec, obtained from photoconductivity decay.[19,20] The decay time of halogen desorption in alkali halides in Table I is of the order of 10^{-3} sec, and again, is much longer than the lifetime of the V_k center at room temperature, 1×10^{-6} sec, obtained by Ueta from transient absorption decay.[21] Furthermore, the data by Ueta suggests a much shorter lifetime of the self-trapped exciton than of the V_k center. These results suggest that the photoexcited species relevant to PSD are not free or self-trapped holes (or excitons), but those having much longer lifetimes. Further discussion on this point will be given in Sec. III D.

In the alkali halides, the decay times observed for alkali atoms are longer than those for halogen atoms, as shown in Table I. This may suggest that the halogen atom is desorbed first and the alkali desorption follows.[2] A possible situation may be that the alkali desorption occurs via an F center near the surface, which is formed by electron capture at halogen vacancies produced by halogen desorption. The process may be similar to the alkali desorption observed under F-band illumination of RbBr containing F centers.[22]

We proceed to discuss the behavior of the silver halides, the desorption kinetics of which is more complicated in comparison to alkali halides. The differences observed between silver and alkali halides are summarized as follows. (1) The desorption decay time τ decreases in increasing excitation intensity I in the silver halides, but remains constant in the alkali halides. (2) "Excitation intensity dependence of the desorption rate" changes with chopping frequency in silver halides: it is proportional to I at high intensity and low frequency and proportional to I^2 at low intensity and high frequency. On the other hand, the desorption rate in the alkali halides is always proportional to I.

These differences may be related to the difference of desorption species between silver and alkali halides, halogen molecules in silver halides, and alkali and halogen atoms in alkali halides, as concluded in Sec. III A. In the

following it will be shown that simple models can explain these features, at least qualitatively.

Suppose that free electron-hole pairs are generated by pulse excitation. The decay kinetics of positive holes can be described by either of the following two models.

1. Model A

The kinetic equation for concentration p of holes without electron-hole recombination or molecule formation will be

$$\frac{dp}{dt}=k_1 I-k_2 p \ , \tag{8}$$

where $k_1 I$ represents the generation rate of holes, I is the absorbed photon flux in quanta/sec, and $k_2 p$ corresponds to a simple decay channel which may be the trapping both at the surface and in the bulk. Assuming that the holes trapped at the surface are instantly desorbed, the desorption rate will be

$$R_{\text{desorp}}=k_2^s p \ , \tag{9}$$

where the superscript s refers to the surface trapping. In the above equations, the concentration p is not necessarily for free holes, but can be for relaxed localized holes which can diffuse in some way.

In the steady-state condition $dp/dt=0$, the desorption rate is proportional to I. During the transient period after pulse excitation, the desorption rate will decay as $p=p_0 e^{-k_2 t}$, where p_0 is the initial concentration proportional to I. Thus the desorption rate in the transient situation is also proportional to I, and the decay time is given by $(1/k_2)$, which is independent of excitation intensity. Model A can describe the features of desorption kinetics in the alkali halides.

2. Model B

Assuming the formation of a diatomic halogen molecule is the dominant decay channel of holes, the kinetic equations are

$$\frac{dp}{dt}=k_1 I-k_2 p^2 \ , \tag{10}$$

$$R_{\text{desorp}}=k_2^s p^2 \ . \tag{11}$$

In the steady state, the desorption rate will be proportional to I. After pulse excitation, the initial decay of the desorption rate can be approximated as

$$R_{\text{desorp}}=k_2^s p_0^2 \exp(-2p_0 k_2 t) \tag{12}$$

within the time range $t \ll 1/p_0 k_2$, where p_0 is the initial concentration at the pulse excitation and is proportional to I. Thus the desorption rate for the initial decay period will be proportional to I^2, and the decay time is $(1/2p_0 k_2)$ which is proportional to I^{-1}.

Model B can explain the features of the desorption kinetics in the silver halides as follows. (1) Decay time decreases in increasing excitation intensity. (2) As for the excitation-intensity dependence, which varies with the range of intensity and frequency, the steady-state condition holds for $(\omega/2\pi)<k_2 p_0$ and the transient situation holds for $(\omega/2\pi)>k_2 p_0$. Then the desorption rate will be proportional to I at high intensity or low frequency and proportional to I^2 at low intensity or high frequency.

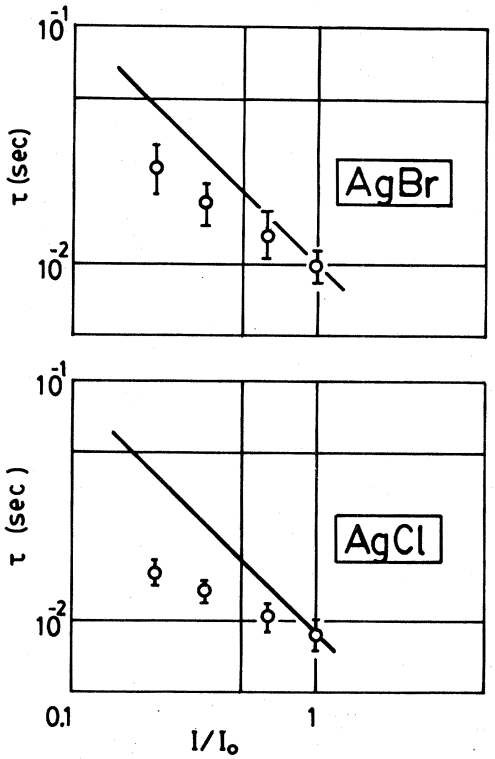

FIG. 7. PSD decay time τ vs excitation intensity for silver halides at 25 °C from the data in Table I.

The decay times shown in Table I for molecular desorption in the silver halides are plotted against excitation intensity in Fig. 7. Compared with the relation $\tau \propto I^{-1}$ expected from Eq. (12), agreement is not exact. Possible origin of the disagreement may be as follows. Firstly, Eq. (12) gives the decay for the initial decay periods, and will be valid for the higher-frequency range in the frequency-dependence data. On the other hand, the decay times obtained from frequency dependence will be an average of steady-state and transient situations. Secondly, model B is too simplified. Actually, Eq. (10) will contain an additional term such as $-kp$ in Eq. (8) representing the trapping of holes at defects. This term will be effective in reducing the decay time in the low-intensity range such as is shown in Fig. 7. In view of the simple nature of model B, the qualitative agreement with features in silver halides in contrast to the alkali halides may be satisfactory.

Summarizing, we succeeded in understanding the origin of different desorption kinetics between silver and alkali halides as being due to the difference in the desorption species identified in Sec. III A. In the silver halides, an additional step of halogen-molecule formation at the surface is required before desorption and this results in the complexities of desorption kinetics compared to the alkali halides.

C. Temperature dependence of desorption yield

With the use of the one-dimensional model for the diffusion of excited species and assuming that the species are desorbed instantly at the surface, the desorption yield for weakly absorbed photons will be proportional to $(D\tau)^{1/2}$, where D is the diffusion coefficient of the species and τ their lifetime.[3,6] Under this condition, the temperature dependence of desorption yield corresponds to that of $(D\tau)^{1/2}$. Combining the data of $(D\tau)^{1/2}$ and τ as a function temperature, we can obtain information on the temperature dependence of D.

Figures 8, 9, and 10 show the temperature dependence of the relative desorption yield for AgBr, AgCl, and RbBr, respectively. The desorption rate under a fixed incident-photon flux is plotted as a function of temperature. Experimental conditions for silver halides were chosen such that the desorption rate is proportional to excitation intensity and the quantum yield can be defined. As suggested from the data in Fig. 5, photoexcitation was given under low chopping frequency, usually 2 Hz, and high photon flux. On the other hand, intermittent photoexcitation was given in all the temperature-dependence measurements, and it was confirmed that the data were not affected noticeably by damage effects due to excessive irradiation. The lifetimes plotted in the figures were obtained from the chopping-frequency dependence obtained in the same way as in Figs. 3 and 4.

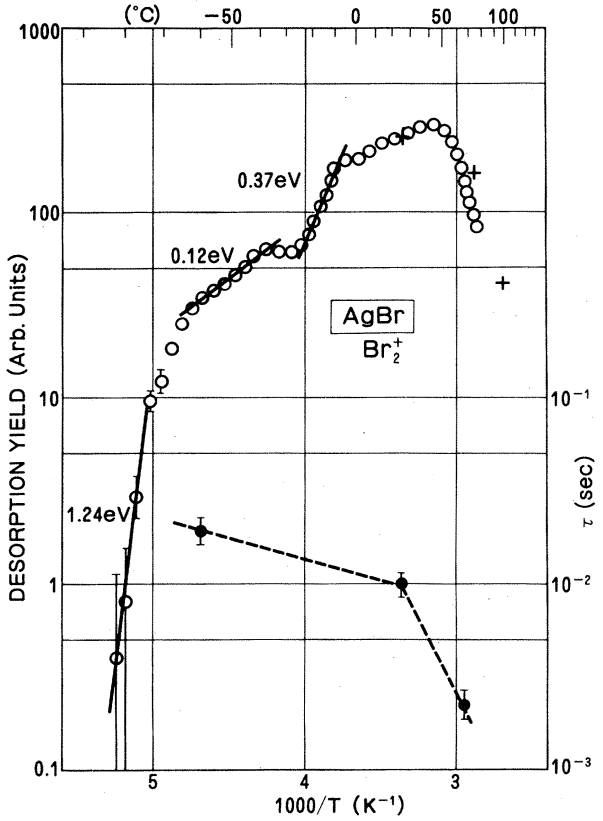

FIG. 8. Temperature dependence of PSD yield for Br_2 molecule and desorption lifetime τ in AgBr. Excitation wavelength is fixed at 360 nm. Pluses are the data by Luckey in Ref. 6 fitted to the scale.

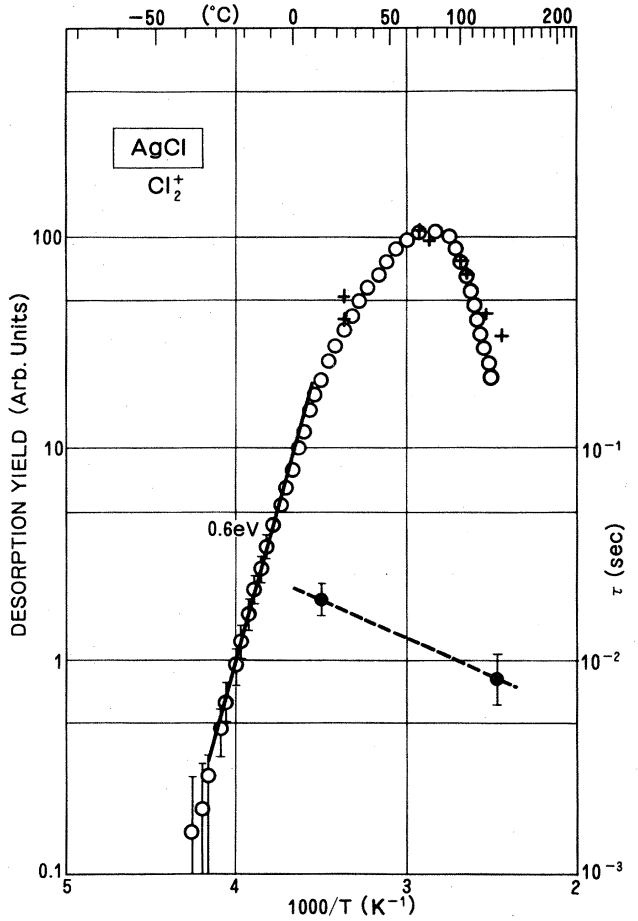

FIG. 9. Temperature dependence of PSD yield for Cl_2 molecule and desorption lifetime τ in AgCl. Excitation wavelength is fixed at 360 nm. Pluses are the data by Luckey in Ref. 6 fitted to the scale.

All the yield data in the low-temperature range exhibit a strong temperature dependence of the thermal activation type. On the other hand, the lifetime is only weakly dependent on temperature, especially in the range where desorption yield increases steeply with temperature. Under this situation, the temperature dependence of desorption yield is mainly determined by that of the diffusion coefficient

$$D = D_0 \exp(-E/k_B T) , \tag{13}$$

and the activation energy of the desorption yield will be $\frac{1}{2}E$ if the above expectation,

$$R_{\text{desorp}} \propto (D\tau)^{1/2} , \tag{14}$$

is valid.

The temperature dependence of Br_2 desorption for AgBr in Fig. 8 starts from the lowest-temperature range with an activation energy of 1.24 eV around −85 °C. The temperature range may correspond to the low-temperature threshold of Br_2 desorption from the surface. This assignment is supported by the observation of the "thermal glow" of Br_2 desorption which peaks at −90 °C when AgBr is rapidly heated after photoirradiation at −120 °C.

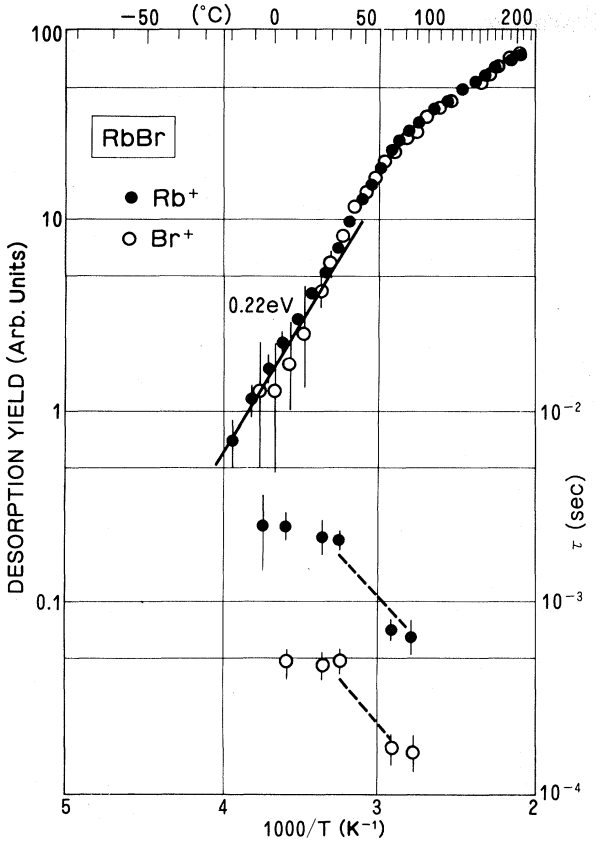

FIG. 10. Temperature dependence of PSD yield for Rb and Br atoms and desorption lifetime τ in RbBr.

Although the photoexcited species produced below −90 °C are mobile and can reach the surface, their desorption requires the energy barrier of 1.24 eV to be overcome. The value of 1.24 eV will correspond to the adsorption energy of Br_2 on the surface of AgBr. Above the temperature of this stage, it can be assumed that the photoexcited species are instantly desorbed as Br_2 when they reach the surface after diffusion from the interior.

The two activation energies, 0.12 and 0.37 eV in Fig. 8, observed at the intermediate-temperature range, can be related to the thermal activation required for the release of excited species from shallow traps. The activation energies nearly twice as large as observed here have been reported in the temperature dependence of the drift mobility of holes. One is the value of 0.20–0.28 eV reported for photoexcited holes between −40 and −60 °C,[19,23] and the other is the value of 0.66–0.71 eV for halogen-injected holes around room temperature.[24,25] These activation energies have been assigned as those required for thermal release of holes from temporarily trapped states. Although the nature of shallow traps is unknown, it seems certain that a similar thermal activation process is operating for diffusion of both the positive holes and the excited species responsible for halogen desorption.

The temperature dependence of Cl_2 desorption for AgCl in Fig. 9 is characterized by a single activation energy of 0.6 eV at low temperature. Very little information is available for the hole diffusion in AgCl and only a preliminary value of activation energy (0.8 eV) has been reported for the diffusion of halogen-injected holes above room temperature.[26] Owing to a lack of information, the nature of the 0.6-eV process in AgCl is not clear.

The temperature dependence of the desorption for RbBr in Fig. 10 is characterized by the activation energy of 0.22 eV for desorption of both Rb and Br. The coincidence of temperature dependence between Rb and Br is consistent with the suggestion in Sec. III B that the alkali desorption is controlled by the halogen desorption. The same activation energy for Rb and Br also suggests that the effect of the surface adsorption energy, such as the 1.24-eV activation energy of AgBr, is unimportant for the desorption from RbBr. The value of 0.22 eV is nearly half of the activation energy (0.41 eV) obtained for the diffusion of self-trapped holes in KBr below room temperature.[21] Although the comparison is not on the same alkali halide, we can reasonably conclude that the diffusion of the self-trapped hole is a controlling factor in the temperature dependence at low temperature.

In the higher-temperature range, the character of the temperature dependence changes. In silver halides, the desorption yield decreases with increasing temperature, namely, above 50 and 80 °C for AgBr and AgCl, respectively (Figs. 8 and 9). In RbBr, the temperature dependence becomes weaker above 80 °C (Fig. 10). A relevant observation follows. Photoexcitation of RbBr for the desorption study is found to produce F centers which are detected by the alkali desorption under excitation of F-band light.[22] However, at temperatures above 100 °C where the temperature dependence becomes weaker, the amount of F centers produced tends to decrease, and finally no F centers remain after photoexcitation above 200 °C. The result suggests that electron-hole recombination becomes dominant in RbBr under excitation above 100 °C. The same situation may be proposed for silver halides in the high-temperature range where thermal quenching of the desorption yield occurs; some of the positive holes recombine with electrons before reaching the surface.

In the case of alkali halides in which the F center is thermally stable in the temperature range concerned, the onset of dominant recombination will be due to the thermal release of trapped holes. In silver halides, the dominant recombination in the high-temperature range was previously ascribed to thermal instability of trapped electrons.[6] However, we prefer the origin as thermal instability of trapped holes on the basis of the following results. In the temperature dependence of PSD for the mixed crystal $AgCl_{0.45}Br_{0.55}$, it is found that the temperature of maximum desorption varies with the desorption species: 5 °C, 30 °C, and 55 °C, for Cl_2, ClBr, and Br_2, respectively.[22] A straightforward interpretation will be that the thermal stability of the desorption precursor varies with species and this is a controlling factor for the onset of dominant recombination. In either case, the observed thermal quenching can be understood as being due to thermal release of trapped states, and its activation energy can be estimated to be 0.6 and 0.7 eV for AgBr and AgCl, respectively, from Figs. 8 and 9.

Summarizing, the temperature dependence of desorption yield in the present study can be understood in terms

of diffusion of photoexcited species. This is one of the features of PSD under excitation near the fundamental absorption edge. Quantitative discussion on the relevant parameters such as D and τ will be given in Sec. III D.

D. Desorption-yield spectra in silver halides

Excitation spectra of relative PSD yield are measured for silver halides in the photon-energy range from fundamental absorption threshold to 5 eV. The spectral range covers the range from the indirect-exciton to the direct-exciton transitions, and the absorption coefficient varies from 2×10^5 cm^{-1} down to 1 cm^{-1}. For such a wide range of absorption strength, an exact treatment of the yield spectrum is required to take account of the diffusion of photoexcited species which are produced in the bulk and diffuse toward the surface with diffusion coefficient D during their lifetime τ.

The following analysis is based on the solution of the one-dimensional diffusion equation under the existence of an "absorbing wall" representing the surface.[18] The absorbing wall is equivalent to assuming that the diffusing species are desorbed instantly when they reach the surface.

Suppose a species is photoexcited in the interior at the depth x from the surface at time $t=0$. The probability $q(x,t)dt$ of the species reaching the surface in the time interval $(t,t+dt)$ is given by[18]

$$q(x,t)dt=\frac{x}{2t(\pi Dt)^{1/2}}\exp\left[\frac{-x^2}{4Dt}\right]dt\ . \tag{15}$$

The total probability $p(x)$ of the species arriving at the surface during its lifetime τ will be

$$p(x)=\int_0^\tau q(x,t)dt=\mathrm{erfc}(x/\lambda\sqrt{2})\ , \tag{16}$$

where

$$\mathrm{erfc}(y)=1-\frac{2}{\sqrt{\pi}}\int_0^y e^{-t^2}dt\ ,$$

and the diffusion length $\lambda=(2D\tau)^{1/2}$. The distribution of photoexcited species produced in the interior depends on the value of absorption coefficient k, and can be expressed by $k\exp(-kx)$ by assuming that the products of photoabsorption are independent of excitation energy. The assumption will be reasonably valid in pure silver halides in the energy region of the present experiment. It has been found that the quantum yield for conduction electrons and holes in silver halides is near unity in the same energy range,[27] and the main products of intrinsic absorption will be free electron-hole pairs irrespective of excitation energy.

Finally, the desorption quantum yield η_{PSD} will be given by,

$$\begin{aligned}\eta_{\mathrm{PSD}}(h\nu)&=k\int_0^\infty \exp(-kx)\mathrm{erfc}(x/\lambda\sqrt{2})dx\ ,\\ &=1-\exp(\lambda^2k^2/2)\mathrm{erfc}(\lambda k/\sqrt{2})\ .\end{aligned} \tag{17}$$

Equation (17) can be easily understood in the limiting cases; η_{PSD} is near unity for the strong-absorption limit of $1/k\ll\lambda$, and $\eta_{\mathrm{PSD}}=k\lambda(2\pi)^{1/2}$ for the weak-absorption limit of $1/k\gg\lambda$. According to Eq. (17), we evaluate $\eta_{\mathrm{PSD}}(h\nu)$ using the experimental value[28] of $k(h\nu)$ and assuming the diffusion length λ.

Figure 11 summarizes typical results of the desorption-yield spectra of AgBr and AgCl at various temperatures. In Fig. 11, experimental data of relative yield (desorption rate in arbitrary units per incident photon) are plotted against incident-photon energy. The values of diffusion length λ are estimated by the best fitting of the data points to Eq. (17), and are summarized in Table II. The quantum-yield spectra calculated from Eq. (17) using the fitted values of λ are shown in Fig. 11 as solid lines. The good agreement of the calculated curves with the data points suggests the following. (1) Although the experimental data are the yields in arbitrary units, the data points can be scaled by the absolute value of quantum yield fitted by Eq. (17), as shown in Fig. 11. This proposi-

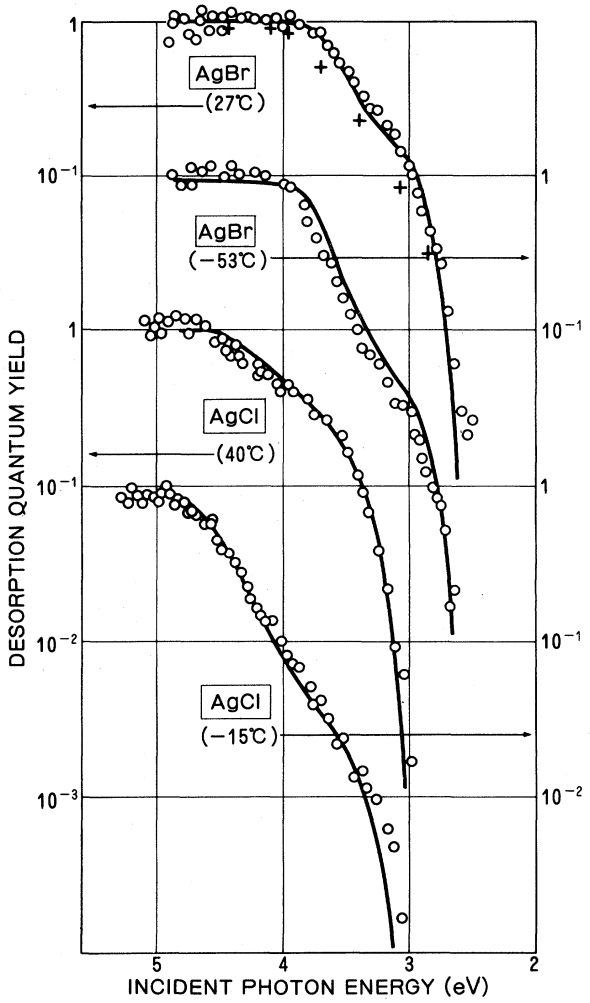

FIG. 11. Desorption-yield spectra in silver halides at various temperatures. Data points are relative yields of halogen-molecule desorption under a chopping frequency of 2 Hz. Solid lines are the quantum yield obtained by fitting the data points to Eq. (17). Pluses are the quantum yield for AgBr estimated from Luckey's data in Ref. 29.

TABLE II. Diffusion length $\lambda=(2D\tau)^{1/2}$ obtained by fitting the desorption-yield spectra of silver halides, such as in Fig. 11, to Eq. (17).

Crystal	Temperature (°C)	λ (10^{-4} cm)
AgBr	27	1.4±0.5
	−11	1.1±0.3
	−53	0.45±0.2
AgCl	40	1.4±0.5
	20	0.7±0.3
	−5	0.2±0.1
	−15	0.14±0.1

tion is supported by the agreement with the quantum yield obtained by Luckey at room temperature,[6,9] as also shown in Fig. 11. (2) The model leading to Eq. (17) is adequate to describe the PSD process in silver halides and can give the value of diffusion length with reasonable accuracy. It is not necessary to assume the change of diffusion length with photon energy which was considered in the previous analysis.[6,29] (3) The quantum yield of PSD can be estimated near unity in the higher-energy range where the absorption coefficient is larger than $1-2\times10^5$ cm^{-1}. This corresponds to the strong-absorption limit mentioned above. The result suggests that PSD is a very efficient channel of relaxation of excited states near the surface.

The temperature dependence of λ shown in Table II is very nearly proportional to that of desorption rate in Sec. III C (Figs. 8 and 9). This indicates that the condition of weak absorption is valid for the photoexcitation in Figs. 8 and 9 because the yield for weak absorption will be proportional to λ as discussed above. The value of λ at room temperature is given as 1×10^{-4} cm in Table II, which is smaller than the inverse of the absorption coefficient $2-3\times10^{-4}$ cm for photoexcitation used in Figs. 8 and 9. The condition of weak absorption is nearly satisfied.

Combining the values of λ and τ obtained in the present study, the diffusion coefficient D can be estimated. For AgBr at room temperature, $(D\tau)^{1/2}\approx1\times10^{-4}$ cm and $\tau\approx1\times10^{-2}$ sec lead to the value of $D\approx1\times10^{-6}$ cm^{2}sec^{-1}. The value is fairly close to $D=3\times10^{-7}$ cm^{2}sec^{-1} obtained by Malinowski[19] for the diffusion of the neutral-hole complex photogenerated in AgBr at room temperature. On the other hand, the values of D obtained for photoexcited free holes are much larger. For example, the drift mobility of photoholes in AgBr at room temperature is 1 cm^{2}V^{-1}sec^{-1},[19,20] which corresponds to $D=3\times10^{-2}$cm^{2}sec^{-1}. We can conclude that the photoexcited species responsible for PSD in AgBr are not free holes but a slow-diffusion species containing holes. They may correspond to the neutral-hole–silver vacancy complexes proposed by Malinowski,[19] at least during a certain period of their lifetime.

It has been confirmed experimentally that the yield spectra in Fig. 11 are free from damage effects due to excessive irradiation. In order to measure the PSD yield spectra of silver halides in the undamaged state, special precautions are found necessary: the excitation photon flux for measurement has to be sufficiently low in order to achieve a reproducible spectral scan. The maximum photon flux used in the data shown in Fig. 11 is 10^{12}–10^{13} quanta cm^{-2}sec^{-1}, and the total exposure for one spectrum scan is order of 10^{15}–10^{16} quanta cm^{-2}. This requirement of using the low photon flux, on the other hand, is contradictory to the requirement for the proportionality of PSD rate to photon flux, as described in Sec. III B. However, it is found that the shape of yield spectra in Fig. 11 does not depend on the magnitude of excitation flux as far as the excitation intensity is sufficiently low and the reproducibility of data is confirmed.

Figure 12 shows typical effects of radiation damage on the yield spectra of AgBr at different temperatures. The change of yield induced by irradiation is more drastic at higher photon energy, and less at lower energy. The result suggests that the exposure-induced effect is confined near the surface, and the PSD yield is selectively influenced by photons with small penetration depth. It is found that the effects such as shown in Fig. 12 can be explained in terms of a modified version of the model outlined above by as-

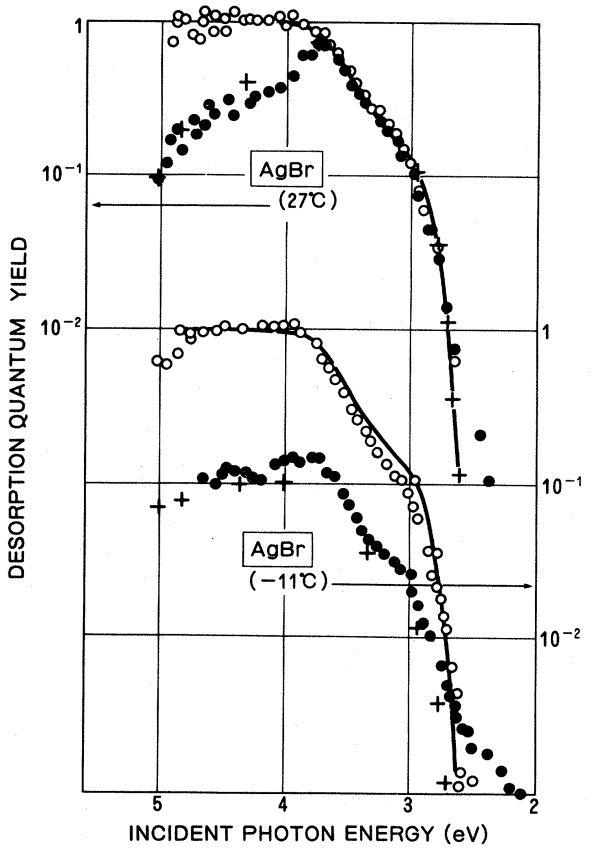

FIG. 12. Typical change of desorption-yield spectra in AgBr due to uv exposure of $\sim10^{17}$ quanta cm^{-2} of 360-nm light at room temperature. Spectra of unexposed sample (○) and after exposure (●) are shown. Pluses are the results of fitting the data after exposure to the surface defect layer characterized by Eq. (18). Solid lines are the quantum yield of the unexposed sample by fitting to Eq. (17).

TABLE III. Parameters of the "surface defect layer" produced by uv exposure in AgBr obtained by fitting the data, such as in Fig. 12, to Eq. (18). λ_0 is the diffusion length before uv exposure.

Temperature (°C)	λ_0 (cm)	λ_0^* (cm)	λ_s (cm)	δ (cm)
27	1.4×10^{-4}	1.4×10^{-4}	1×10^{-7}	7×10^{-7}
−11	1.1×10^{-4}	1.4×10^{-5}	4×10^{-7}	17×10^{-7}
−40	0.45×10^{-4}	0.45×10^{-5}	0.5×10^{-7}	3×10^{-7}

suming the existence of "defect layer" near the surface produced by irradiation. As a simple model convenient for calculation, we assume the defect layer of thickness δ near the surface, and express the distribution of diffusion length λ in the damaged sample as

$$1/\lambda = 1/\lambda_0^* + (1/\lambda_s - 1/\lambda_0^*)\exp(-x/\delta)\,, \tag{18}$$

where λ_0^* is the diffusion length far from the surface, λ_s is the diffusion length at the surface, and x is the distance from the surface. The desorption quantum yield is numerically calculated by assuming that Eq. (18) and the best-fitted results are shown in Fig. 12. The corresponding parameters are summarized in Table III.

The results indicate the following properties of radiation-induced defects in AgBr. (1) The effects on PSD yield are more drastic at lower temperature as shown in Fig. 12. (2) Diffusion length in the bulk is reduced at low temperature but not at room temperature, as shown in Table III. (3) Tailing of yield spectra is observed at low energies, as shown in Fig. 12. It can be suggested that the irradiation produces various defects near the surface and in the interior which have a variety of thermal binding energies in trapping the photoexcited species responsible for PSD. A possible candidate for the defects may be the silver clusters which are shown to present an extra PSD yield in the lower-energy region.[10]

Summarizing, the excitation spectra of PSD yield in silver halides are successfully analyzed in terms of the diffusion of photoexcited species to the surface. The diffusion coefficient of the excited species is found to be far smaller than that of free holes, and the diffusion of neutral species containing holes is suggested. The effects of irradiation on yield spectra are explained by the formation of defects dominantly near the surface.

IV. SUMMARY

Results of the present study will be summarized in terms of the three-step model for the PSD process.[11] In the first step, excited states are produced in the bulk by optical excitation. They diffuse toward surface in the second step, and finally, in the third step, desorption occurs at the surface.

In the first step of PSD, the excited states produced by low-energy valence excitation, such as in the present study, will be either free excitons or free electron-hole pairs. In the silver halides, free excitons dissociate efficiently near room temperature and the main products are free electron-hole pairs. In the alkali halides, on the other hand, free excitons are mainly produced in the present study.

The nature of the excited states changes in going from the first to the second step of PSD. The excited states in the silver halides responsible for halogen desorption will contain positive holes. However, the diffusing species in AgBr are not free holes such as produced in the first step, but neutral-hole complexes which diffuse more slowly and have a longer lifetime in comparison to free holes. Self-trapped holes are stable in AgCl at low temperature, but thermally delocalized[10] in the temperature range of the present study. The diffusing species in AgCl may be similar to those in AgBr as far as their diffusion coefficient and lifetime are concerned.

The diffusing species for halogen desorption in alkali halides have a much longer lifetime than V_k centers (self-trapped holes) and the activation energy for diffusion is near that of V_k centers. The diffusion of a V_k center through intermittent capture at point defects may correspond to the situation.

The third step of PSD requires an activation energy for the evaporation of the precursor state from the surface. The magnitude of the activation energy determines the main PSD species, which are identified as halogen molecules in silver halides, and alkaki-metal and halogen atoms in the alkali halides. The difference in species, either of molecular or atomic nature, leads to the differences in desorption kinetics between the silver and alkali halides. In AgBr, the low-temperature threshold of desorption is determined by the surface-desorption process. In AgCl and RbBr, on the other hand, the low-temperature threshold is determined by the diffusion process of the excited states.

The excitation spectra of the desorption yield in silver halides are successfully analyzed by the diffusion of excited states toward the surface. The diffusion length thus estimated, in combination with the desorption lifetime, gives the diffusion coefficient of photoexcited states from which the nature of the diffusing species is suggested.

From the experimental results in the present study, it can be concluded that the diffusion of photoexcited states toward the surface is important in understanding the PSD process under low-energy valence excitation.

ACKNOWLEDGMENTS

This work was partially supported by a Grant-in-Aid for Scientific Research from the Ministry of Education (Japan) and by research grants from Toray Science Foundation and Fuji-Film Research Laboratories.

[1]D. Menzel, J. Vac. Sci. Technol. 20, 538 (1982).
[2]P. D. Townsend, R. Browning, D. G. Garlant, J. C. Kelly, A. Mahjoobi, A. J. Michael, and M. Saidoh, Radiat. Eff. 30, 55 (1976).
[3]H. Overeijnder, M. Szymoński, A. Haring, and A. E. deVries, Radiat. Eff. 36, 63 (1978); 38, 21 (1978).
[4]N. Itoh, Nucl. Instrum. Methods 132, 201 (1976).
[5]A. Schmid, P. Bräunlich, and P. K. Rol, Phys. Rev. Lett. 35, 1382 (1975).
[6]G. W. Luckey, J. Phys. Chem. 57, 791 (1953); 23, 882 (1955).
[7]N. H. Tolk, L. C. Feldman, J. S. Kraus, R. J. Morris, M. M. Traum, and J. C. Tully, Phys. Rev. Lett. 46, 134 (1981); N. H. Tolk, M. M. Traum, J. S. Kraus, T. R. Pian, W. E. Collins, N. G. Stoffel, and G. Margaritondo, *ibid.* 49, 812 (1982).
[8]M. L. Knotek and P. J. Feibelman, Phys. Rev. Lett. 40, 964 (1978).
[9]M. L. Knotek, Semicond. Insulators 5, 361 (1983); F. J. Himpsel, *ibid.* 5, 419 (1983).
[10]H. Kanzaki, Semicond. Insulators 3, 285 (1978); 5, 517 (1983); Y. Toyozawa, *ibid.* 5, 175 (1983).
[11]H. Kanzaki and T. Mori, Semicond. Insulators 5, 401 (1983).
[12]P. W. Palmberg and T. N. Rhodin, J. Phys. Chem. Solids 29, 1917 (1968); A. Friedenberg and Y. Shapira, Surf. Sci. 87, 581 (1979).
[13]H. Kanzaki and S. Sakuragi, J. Phys. Soc. Jpn. 27, 109 (1969); 29, 924 (1970).
[14]L. A. Larsen, T. Oda, P. Bräunlich, and J. T. Dickinson, Solid State Commun. 32, 347 (1979).
[15]M. Szymoński, H. Overeijnder, and A. E. deVries, Surf. Sci. 90, 274 (1979).
[16]R. G. Copperthwaite and M. Steinberg, Solid State Commun. 28, 915 (1978).
[17]H. Overeijnder, R. R. Tol, and A. E. deVries, Surf. Sci. 90, 265 (1979).
[18]S. Chandrasekhar, Rev. Mod. Phys. 15, 1 (1943).
[19]J. Malinowski, Contemp. Phys. 8, 285 (1967); J. Photogr. Sci. 16, 57 (1968).
[20]V. J. Saunders, R. W. Tyler, and W. West, J. Chem. Phys. 37, 1126 (1962).
[21]M. Ueta, J. Phys. Soc. Jpn. 23, 1265 (1967).
[22]H. Kanzaki and T. Mori (unpublished).
[23]R. K. Ahrenkiel and R. S. Van Heyningen, Phys. Rev. 144, 576 (1966).
[24]G. W. Luckey, Discuss. Faraday Soc. 28, 113 (1959).
[25]E. Eisenmann and W. Jaenicke, Z. Phys. Chem. Neue Folge 49, 1 (1966).
[26]P. Müller, S. Spenbe, and J. Teltow, Phys. Status Solidi 41, 81 (1970).
[27]V. I. Saunders, R. W. Tyler, and W. West, Photogr. Sci. Eng. 16, 87 (1972).
[28]H. Kanzaki, Photogr. Sci. Eng. 24, 219 (1980).
[29]V. I. Saunders, J. Opt. Soc. Am. 67, 830 (1977).